Electronic Supplementary Information

Dithiocarbamate-capped silver nanoparticles as a resonance light scattering probe for simultaneous detection of lead(II) ions and cysteine

Haiyan Cao,[a] Minghong Wei,[a] Zhaohui Chen,*[a,b] Yuming Huang*[a]

[a] *State Key Laboratory Breeding Base of Eco-Environments and Bio-Resources of the Three Gorges Reservoir Region; College of Chemistry and Chemical Engineering, Southwest University, Chongqing 400715, China.*
E-mail: ymhuang@swu.edu.cn
[b] *Basic Department of Rongchang Campus, Southwest University, Chongqing 402460, China. E-mail: zhaohuic@swu.edu.cn*

Table S1. The effect of Pb^{2+} concentration on the hydrodynamic diameter and surface charges of the DTC-Ag NPs.

Concentration of Pb^{2+} (µM)	Average particle size (nm)	Zeta Potential (mV)
0	26.95	-46.7
1	28.88	-34.6
10	246.1	-26.7
100	1024.8	19.1

Table S2. The effect of cysteine concentration on the hydrodynamic diameter and surface charges of the DTC-Ag NPs in the presence of 20 µM Pb^{2+}.

Concentration of cysteine (µM)	Average particle size (nm)	Zeta Potential (mV)
0	298.5	-18.7
0.2	186.1	-21.7
2	168.5	-27.2
20	41.4	-32.7

Table S3 LOD comparison of this work with some established methods for Pb^{2+}

System	Detection limit (μM)	Analytical methods	References
Thiol-capped CdTe QDs	0.27	Fluorescence	1
Glutathione-functionalized Au NPs	0.1	Colorimetric	2
DNAzyme-functionalized Au NPs	0.1	Colorimetric	3
Pentapeptide-Au NPs	0.1	Colorimetric	4
Gallic acid-Au NPs	0.025	Colorimetric	5
Functionalized fluorescent Au NDs	0.002	Fluorescence	6
Podand triazole-linked Au NPs	7	Colorimetric	7
Gallic acid-Au NPs or Ag NPs	5	Colorimetric	8
dsDNA-Cu NPs	0.005	Fluorescence	9
di-(2-picolyl) amine (DPA) substituted diacetylene	4	Fluorescence	10
Ammonium molybdate	0.009	Light scattering	11
Sodium tetraphenylboron-polyethylene glycol	0.013	Light scattering	12
DEA-Ag NPs	0.004	Light scattering	this work

References

1. H. M. Wu, J. G. Liang and H. Y. Han, *Microchim. Acta*, 2008, **161**, 81-86.
2. F. Chai, C. Wang, T. Wang, L. Li and Z. Su, *ACS Applied Materials & Interfaces*, 2010, **2**, 1466-1470.
3. J. Liu and Y. Lu, *J. Am. Chem. Soc.*, 2003, **125**, 6642-6643.
4. Z. X. Wang and X. K. Li, *Chem Res Chinese U*, 2010, **26**, 194-197.
5. N. Ding, Q. Cao, H. Zhao, Y. Yang, L. Zeng, Y. He, K. Xiang and G. Wang, *Sensors-Basel*, 2010, **10**, 11144-11155.
6. Z. Yuan, M. Peng, Y. He and E. S. Yeung, *Chem. Commun.*, 2011, **47**, 11981-11983.
7. H. Li, Q. Zheng and C. Han, *Analyst*, 2010, **135**, 1360-1364.
8. K. G. Thomas, K. Yoosaf, B. I. Ipe and C. H. Suresh, *J. Phys. Chem. C*, 2007, **111**, 12839-12847.
9. J. Chen, J. Liu, Z. Fang and L. Zeng, *Chem. Commun.*, 2012, **48**, 1057-1059.
10. K. M. Lee, X. Chen, W. Fang, J.-M. Kim and J. Yoon, *Macromol. Rapid Commun.*, 2011, **32**, 497-500.
11. Y. Cui, F. Cui, L. Wang, Q. Zhang, W. Xue, F. Jing and J. Sun, *J. Lumin.*, 2008, **128**, 1719-1724.
12. K. J. Tan, C. Z. Huang and Y. M. Huang, *Talanta*, 2006, **70**, 116-121.
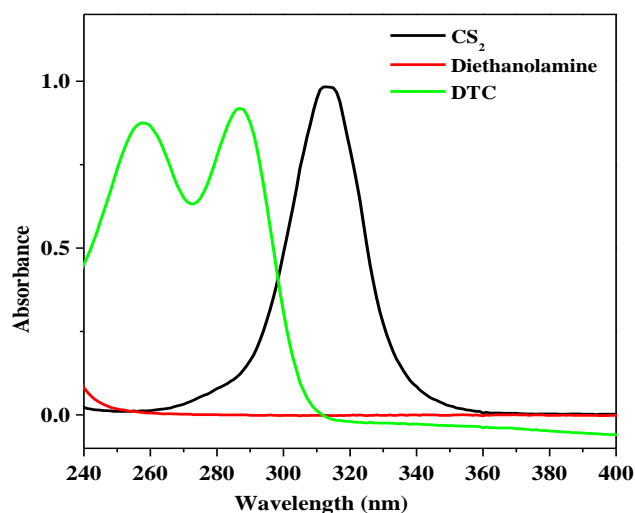

Figure S1. UV absorption spectra of CS_2, diethanolamine, and mixture of CS_2 and diethanolamine (after 1 min mixing under sonication).
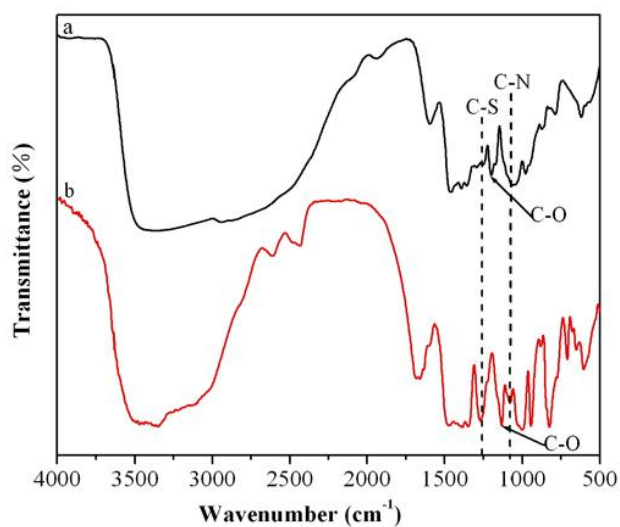
Figure S2. FTIR spectra of (a) DTC; (b) DTC-Ag NPs.

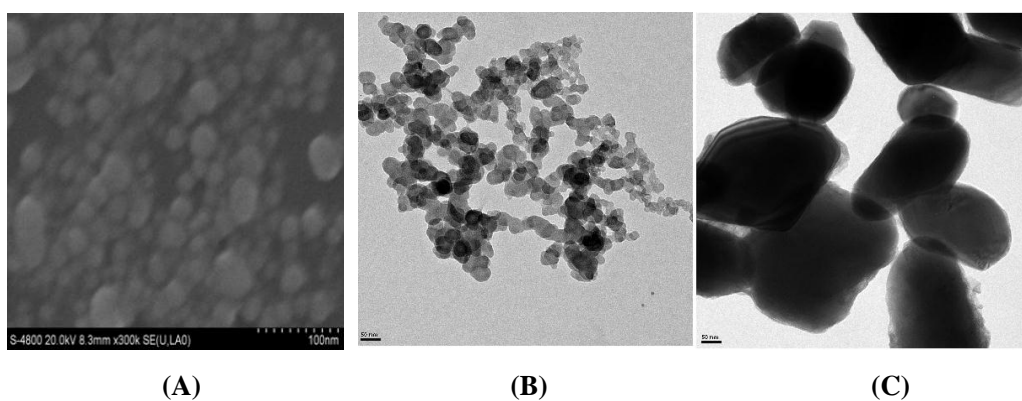

(A)   **(B)**   **(C)**

Figure S3. (A) SEM image of DTC-Ag NPs (scale bar corresponds to 100 nm). TEM images of DTC-Ag NPs without (B) and with (C) Pb^{2+} (scale bar corresponds to 50 nm).
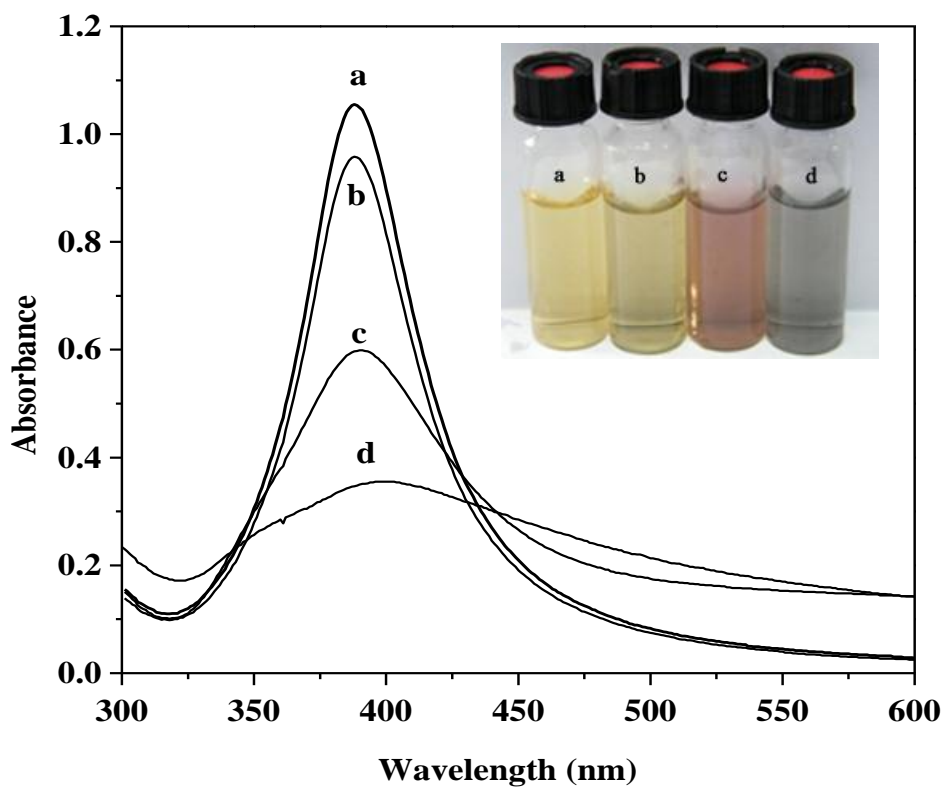
4

Figure S4. UV-Vis absorption spectra of the DEA-Ag NPs (8.64 mg L^{-1} as Ag) solution at different concentration of Pb^{2+}: (a) 0 μM; (b) 1 μM; (c) 5 μM; (d) 20 μM. Inset: The color change with different concentration of Pb^{2+}.
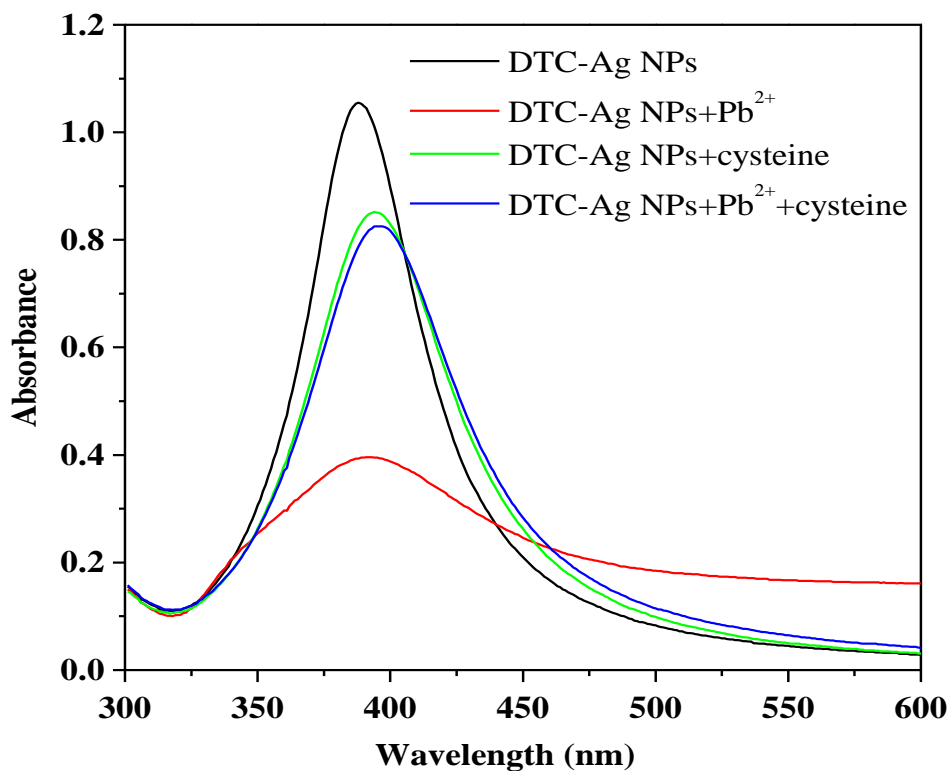
Figure S5. UV-Vis absorption spectra of the DEA-Ag NPs- Pb^{2+} system at different concentration of cysteine. Reaction conditions: 8.64 mg L^{-1} DEA-Ag NPs (as Ag), 10 μM Pb^{2+}, and 10 μM cysteine.
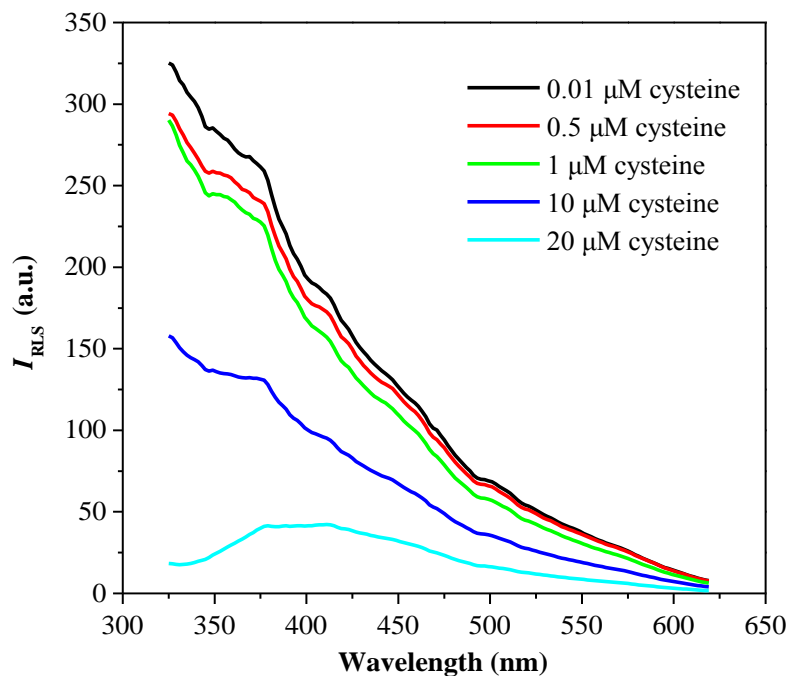

Figure S6. The RLS spectra of DTC-Ag NPs (648 μg L^{-1} as Ag)-Pb^{2+} system with various concentrations of cysteine (0.01, 0.5, 1, 10, and 20 μM, respectively).
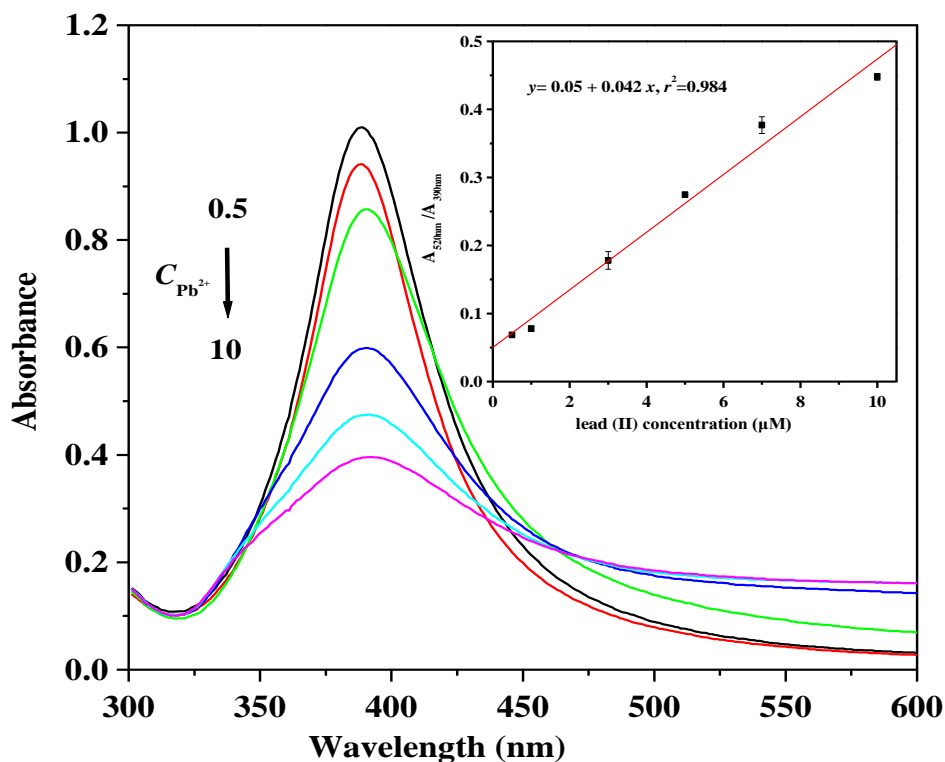
Figure S7. The absorbance spectra of DTC-Ag NPs (8.64 mg L^{-1} as Ag) with addition of various concentrations of Pb^{2+} (0.5, 1, 3, 5, 7, 10 μM, respectively). The inset is linear calibrated curve for Pb^{2+}.
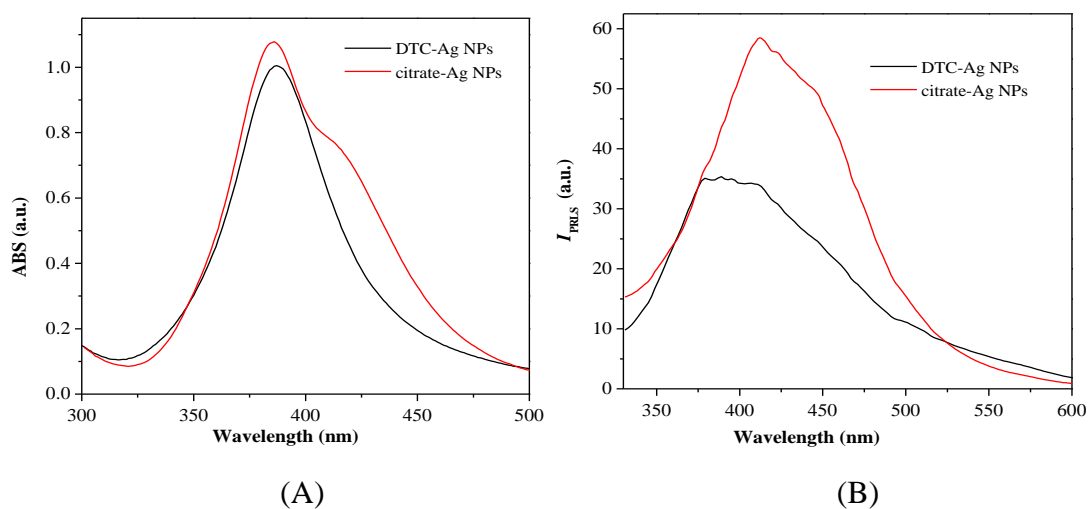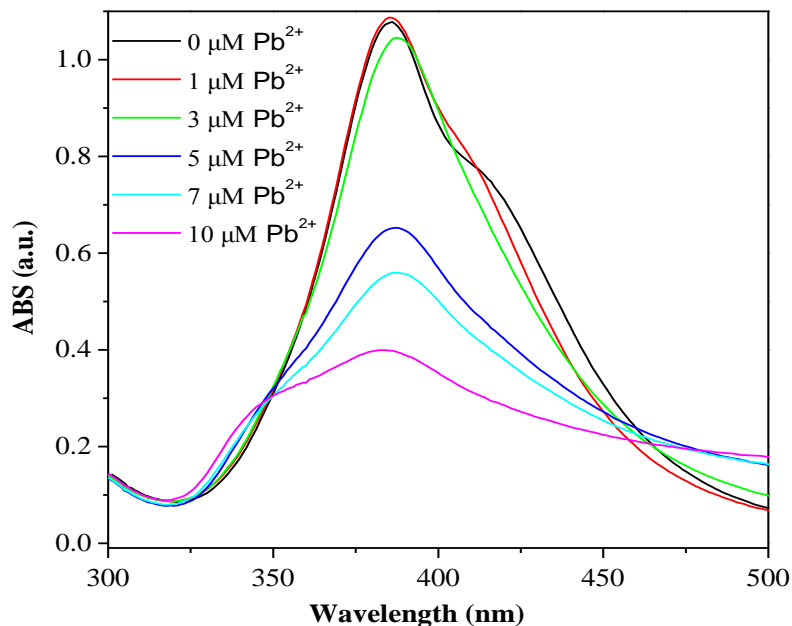

(A)

(B)

Figure S8. (A) UV-Vis absorption spectra of the DTC-Ag NPs (8.64 mg L^{-1} as Ag) solution and the citrate-AgNPs (8.64 mg L^{-1} as Ag). (B) The RLS spectra of DTC-Ag NPs (648 μg L^{-1} as Ag) solution and the citrate-AgNPs (648 μg L^{-1} as Ag).

Figure S9. The absorbance spectra of citrate-Ag NPs (8.64 mg L^{-1} as Ag) with addition of various concentrations of Pb^{2+} (0, 1, 3, 5, 7, 10 μM, respectively).
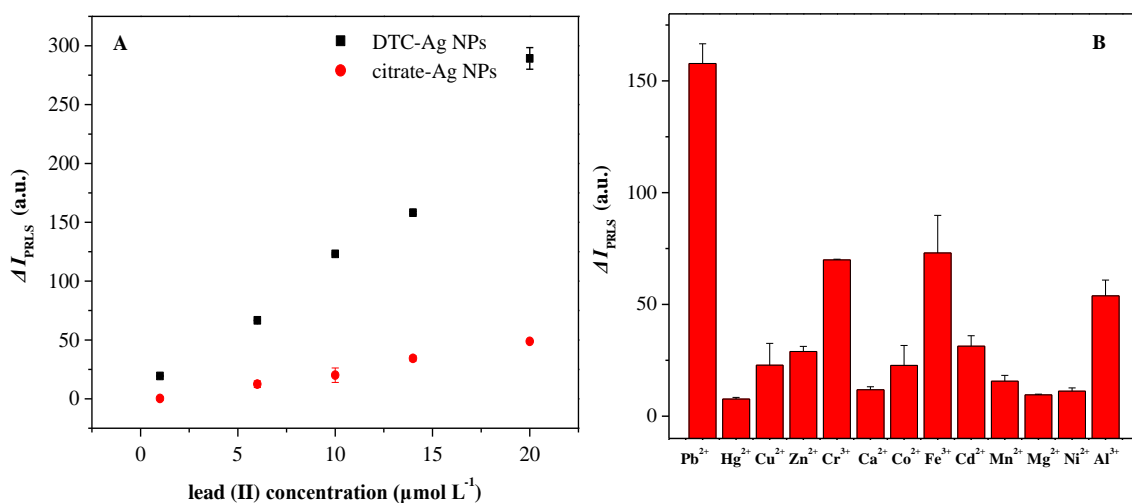

Figure S10. (A) The net RLS intensity of DTC-Ag NPs (black square) with addition of various concentrations of Pb^{2+} (1, 6, 10, 14, and 20 μM) and citrate-Ag NPs (red dot) with addition of various concentrations of Pb^{2+} (1, 6, 10, 14, and 20 μM). (B) Selectivity of the citrate-Ag NPs-based RLS probe for Pb^{2+} over other ions. Concentrations of citrate-Ag NPs and Pb^{2+} were 0.65 mg L^{-1} and 60 μM respectively; concentrations of all other metal ions were 60 μM. Error bars represent one standard deviation for three measurements.
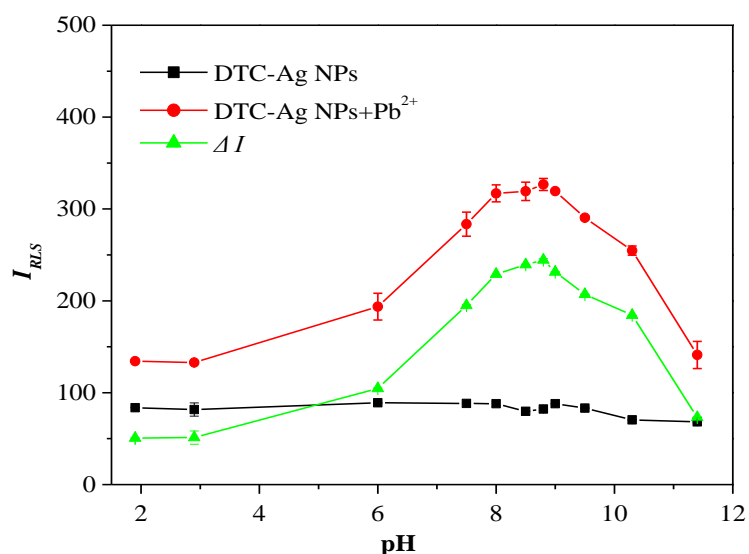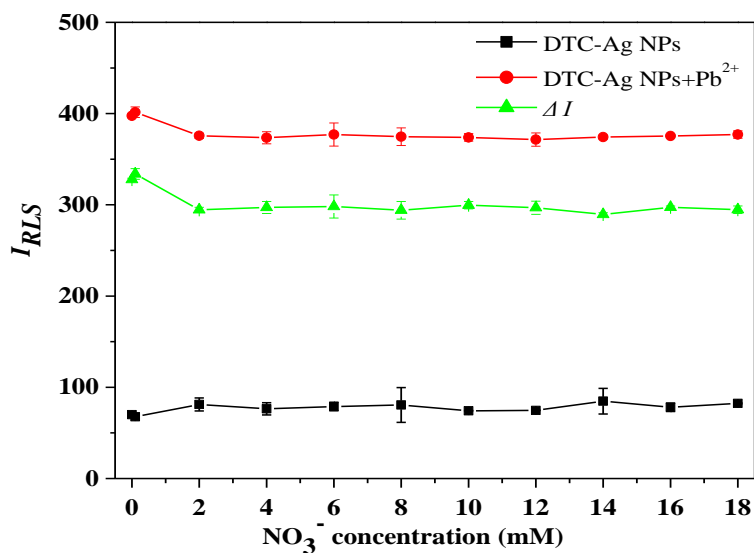
Figure S11. Effect of pH on RLS intensity of DTC-Ag NPs with and without Pb^{2+}.

Reaction conditions: DTC-Ag NPs concentration: 1.73 mg L^{-1} (as Ag); Pb^{2+}

concentration: 20 μM. Error bars represent one standard deviation for three

measurements.

Figure S12. Effect of salinity on RLS intensity of DTC-Ag NPs with and without

Pb^{2+}. Reaction conditions: DTC-Ag NPs concentration: 1.73 mg L^{-1} (as Ag); Pb^{2+}

concentration: 20 μM. Error bars represent one standard deviation for three
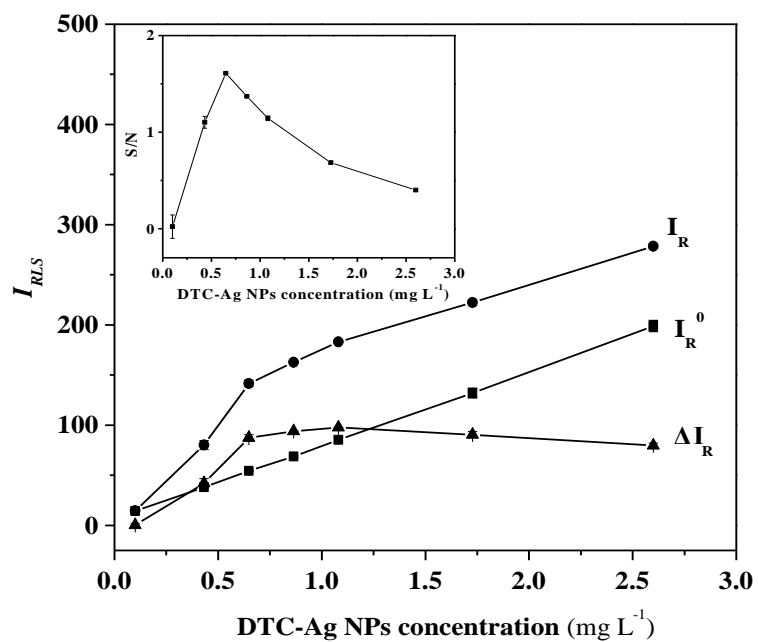
measurements.

9

Figure S13. Effect of DTC-Ag NPs concentration. Pb^{2+} concentration: 6 μM. Error bars represent one standard deviation for three measurements.

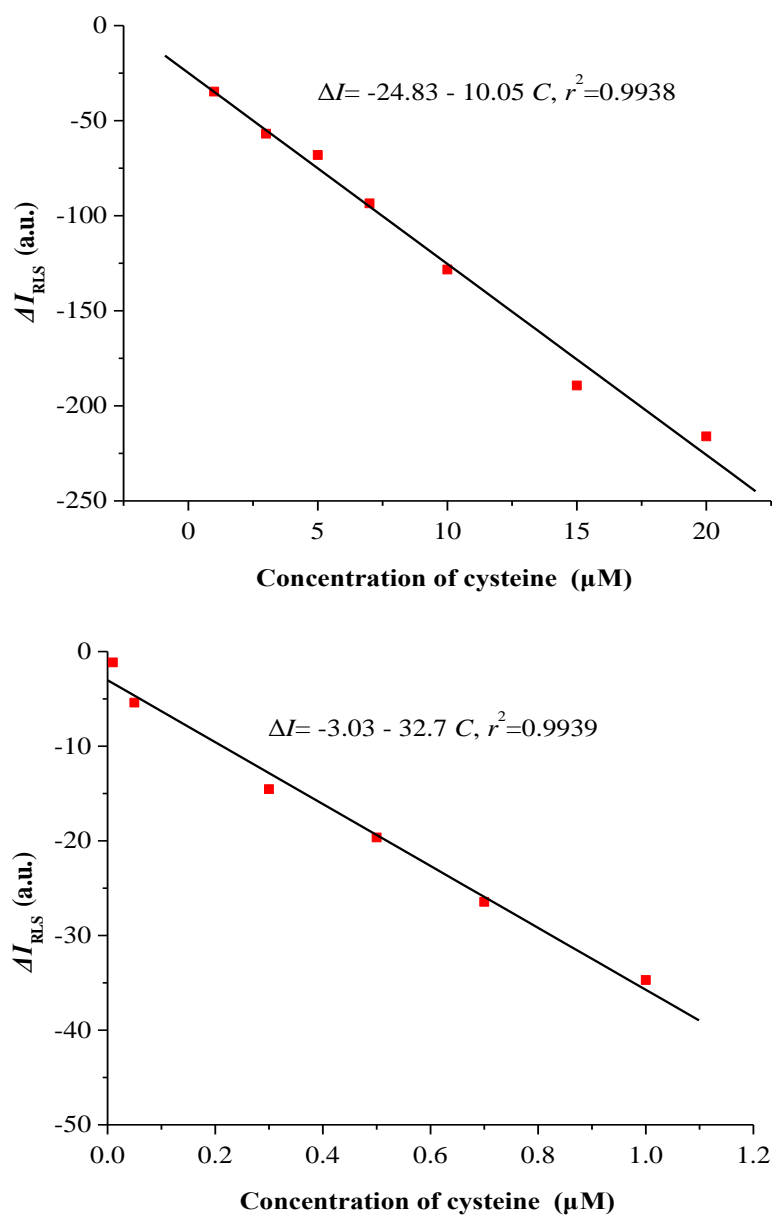$\Delta I = -24.83 - 10.05\ C,\ r^2 = 0.9938$

$\Delta I = -3.03 - 32.7\ C,\ r^2 = 0.9939$

Figure S14. The response curves of cysteine.